2E5-1

Proceedings of Symposium on Ultrasonic Electronics, Vol. 35 (2014) pp. 369-370
3-5 December, 2014

Brillouin scattering and first principle studies of relaxor ferroelectric $44Pb(Mg_{1/3}Nb_{2/3})O_3$-$56PbTiO_3$

ブリルアン散乱と第一原理計算によるリラクサー強誘電体 $44Pb(Mg_{1/3}Nb_{2/3})O_3$-$56PbTiO_3$ の研究

Helal Md Al‡ and Seiji Kojima
PAS, Univ. of Tsukuba, Tsukuba, Ibaraki 305-8573, Japan
Helal Md Al‡, 小島誠治　(筑波大)

1. Introduction

There has been a great deal of interest in a new class of relaxor-based ferroelectric perovskite $Pb[(Mg_{1/3}Nb_{2/3})_{1-x}Ti_x]O_3$ (PMN-*x*PT) due to their superior piezoelectric properties [1] compared to the conventional $PbZr_xTi_{(1-x)}O_3$ ceramics that have dominated piezoelectric applications for last several decades. Since their discovery early in 1959's [2], there have been extensive theoretical and experimental studies [1,3,4] which greatly advanced our understanding of relaxors. However, the mechanism of underlying the ultrahigh performance of these materials and consequently the possibility of further improvements of relaxors still remain unclear.

Knowledge of elastic constants helps us to better understanding the role of electromechanical response of a material under applied stress and fields. Elastic properties can be determined by using various methods such as ultrasonic pulse-echo/resonance or Brillouin scattering techniques, depending on the availability of single crystals of appropriate size. Brillouin scattering is the non-contact method, which enables the measurement of the large temperature range. In addition, recently a complete set of elastic, piezoelectric and dielectric properties of PMN-*x*PT of several compositions has been reported [5]. In the present study, we have reported the elastic properties of $0.44Pb(Mg_{1/3}Nb_{2/3})O_3$-$0.56PbTiO_3$ (PMN-56PT) single crystal by using the micro-Brillouin scattering technique in back scattering geometry [6]. To extract the elastic constants of PMN-56PT, we have also performed the first principle study using pseudopotential technique. Our calculated results are then compared with Brillouin scattering results, which shows a good agreement between theory and experiment.

2. Experimental

E-mail address: helalphy82@gmail.com

The PMN-56PT single crystals were grown by the Bridgeman method. An excitation light source was a diode pumped solid state laser at the wavelength of 532 nm. The scattered light was analyzed by a micro-Brillouin scattering system with a 3+3 pass Sandercock-type tandem Fabry-Pérot interferometer with a photon-counting system [6].

3. Theoretical Methodology

We have performed the first-principle calculations based on the density functional theory (DFT) as implemented in CASTEP (Cambridge Sequential Total Energy Package) code [7]. On the fly pseudopotential was employed to indicate the interaction between the ionic cores and valence electrons. The calculations are performed using the local density approximation (LDA) with CA-PZ functions. The *k* points were set at 3×3×3 with the cut-off energy values of the plane wave expansions in 610 eV after convergence test.

4. Results and Discussion

Figure 1 shows a set of typical Brillouin spectra at a few selected temperatures in the present backward scattering geometry. One pair corresponds to the longitudinal acoustic (LA) mode and another pair corresponds to the transverse acoustic (TA) mode. The sound velocity $V_{\mathrm{LA/TA}}$ and the elastic stiffness constant C_{ij} have been calculated according to the following equations:

$$V_{\mathrm{LA/TA}} = \frac{\lambda \upsilon_B}{2n} \quad \cdots\cdots(1)$$

$$C_{11} = \rho V_{LA}^2 \quad \cdots\cdots(2)$$

$$C_{66} = \rho V_{TA}^2 \quad \cdots\cdots(3)$$

$$C_{44} = \rho V_{TA}^2 \quad \cdots\cdots(4)$$

where, λ and n are the wavelength of the laser light (532 nm in the present case) and the refractive index at λ. J.H. Co *et al.* [8], reported the refractive index of PMN-55PT single crystal is 2.61 at the wavelength of 532 nm. The density

Table I. Elastic stiffness constants C_{ij} (GPa) obtained from Brillouin spectroscopy compared with DFT calculations for PMN-56PT at 25°C and 350°C in both the tetragonal and cubic phases, respectively.

Elastic constants	Tetragonal phase		Cubic phase	
	DFT	Brillouin scattering	DFT	Brillouin scattering
C_{11}	227.8±3.4	229.6	198.9±1.7	208.04
C_{12}	79.3±1.3		87.3±1.3	
C_{44}	51.8±5.7		73.4±1.2	86.79
C_{13}	65.3±1.6			
C_{33}	106.9±13.2			
C_{66}	83.6±0.8	88.9		

was determined from the extrapolated value of density obtained in ref. 5.

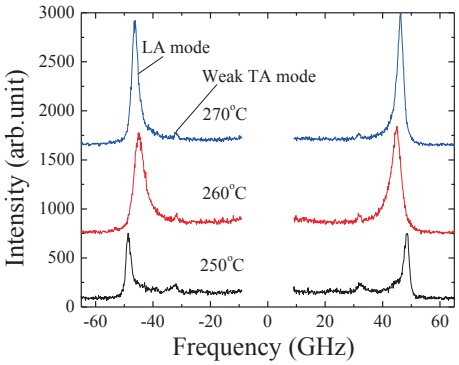

Fig. 1 Brillouin scattering spectra at three selected temperatures of PMN-56PT.

With decreasing temperature, the elastic constant C_{11} shows marked softening towards the cubic-tetragonal phase transition temperature ($T_{C\text{-}T}$~260°C) as shown in **Fig.2**.

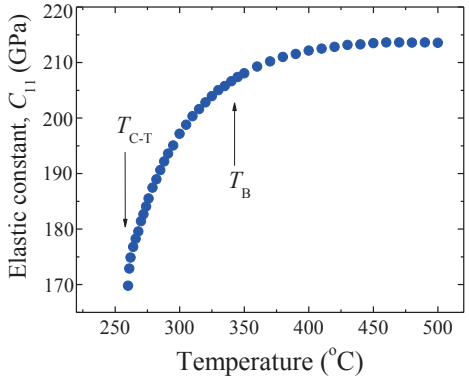

Fig. 2 Temperature dependence of elastic constant, C_{11} of PMN-56PT.

The plot of the derivative of LA shift shows the clear deviation at about 340°C from linear temperature dependence and is assigned as Burns temperature (T_B), where the formation of dynamic polar nanoregions (PNRs) begins. The temperature dependence of elastic constant C_{11} shows a clear deviation at about 340°C from the linear temperature dependence as shown in Fig.2. It can be attributed to coupling between the fluctuating PNRs and LA mode.

To discuss our Brillouin scattering results, we have performed the first-principle calculations based on the DFT as implemented in CASTEP code. In the case of tetragonal phase, there are six independent elastic stiffness constants C_{ij} i.e., C_{11}, C_{12}, C_{13}, C_{33}, C_{44}, and C_{66}. And in the case of cubic phase there are three independent elastic stiffness constants i.e. C_{11}, C_{12}, and C_{44}. These constants have been calculated and displayed in **Table 1** in comparison with Brillouin scattering results. Our calculated values of elastic constants show good agreement with the observed one within experimental uncertainty.

5. Acknowledgement

The authors are grateful to Mr. Matsumoto and Mr. Rahman for their support of Brillouin scattering measurement and discussion.

References

[1] S.-E. Park and T.R. Shrout: J. Appl. Phys. 82 (1997)1804.
[2] G.A. Smolenskii and A.I. Agranoskaya: Sov. Phys. Solid State 1(1959)1421.
[3] Z.G. Ye: Key Eng. Mater. 155 (1998)81.
[4] H.Fu and R.E. Cohen: Nature 403(2000)281.
[5] H. Cao, V. H. Schmidt, R. Zhang, W. Cao and H. Luo: J. Appl. Phys. 96(2004)549.
[6] S. Kojima: Jpn. J. Appl. Phys. 49 (2010) 07HA01.
[7] M.D. Segal, P.J.D. Lindan, M.J. Probert, C.J. Pickard, P.J. Hasnip, S.J. Clark, M.C. Payne: J.Phys.: Condens. Matter 14 (2002) 2717.
[8] J.H.Co, T.H. Kim, S. Kojima, A.A. Bokov,and Z.G. Ye: J.Phys.: Condens. Matter 22(2010) 485902.